Chapter

Terahertz Sensing Based on Photonic Crystal Fibers

Md. Ahasan Habib, Md. Shamim Anower and Md. Nazmul Islam

Abstract

Photonic-crystal-fiber (PCF) based sensors in the terahertz spectrum have been immensely studied and implemented due to their unique advantages and high sensitivity. At an early stage, conventional and hybrid structured porous core PCF-based sensors were proposed, but the sensitivity was not so high. With the advancement of PCF fabrication technology, hybrid structured hollow-core PCFs have been reported and offer superior sensing characteristics than the previous types. In this chapter, both porous core and hollow-core PCF-based THz sensors are analyzed and the propagation characteristics are explained using terahertz spectrum. Finally, some promising terahertz sensors are studied and compared at the end of this chapter.

Keywords: terahertz, photonic crystal fiber, relative sensitivity, porous & hollow-core PCF

1. Introduction

The electromagnetic signal whose frequency ranges between 0.1 and 10 THz is termed the terahertz radiation band [1–4]. This radiation band has been effectively used in numerous applications, such as sensing, medical imaging, biotechnology, and genetic engineering, security, chemical spectroscopy, diagnosis of different cancerous cells, radar, and astronomy [5–10]. Due to the massive advancement in the optoelectronics sector, numerous types of terahertz sources and terahertz detectors (photoconductive antennas, bolometers, *etc*.) are already available on the market [11–13]. On the contrary, efficient and favorable terahertz waveguides are still under research. The major barrier for the expansion of terahertz waveguides in different applications is the selection of waveguide base material. Metallic waveguides are suitable for microwave signal propagation, but they offer high ohmic loss for higher frequency signals. A circular-shaped metallic waveguide [14] was proposed in 1999, which suffered only ohmic loss for terahertz signals, whereas coplanar and microstrip transmission lines exhibited other types of losses [15]. One of the major drawbacks of this circular waveguide was the strong dispersion near the cut-off frequency. One year later, a rectangular metallic waveguide [16] was demonstrated theoretically and experimentally, which experienced the same type of loss and dispersion problem as the circular metallic waveguide [15]. In 2001, a copper-based parallel plate terahertz waveguide was proposed, which exhibited only ohmic loss but the dispersion was absent for this type of waveguide [17]. After that, Wang

and Mittleman first introduced bare metal or Sommerfeld wire as a terahertz waveguide, and they proved that this waveguide offered less loss than the metallic waveguides [18]. However, in metallic waveguides, the ohmic loss was low, but this waveguide experienced fewer light confinement problems for terahertz waves. This problem can be solved by replacing metallic slit waveguides instead of the bare metal waveguide, and it was first introduced in 2007 [19]. Along with the various types of metallic waveguides, some remarkable dielectric waveguides were also proposed by the researchers, which also include those in the terahertz frequency range. The dielectric waveguides were used to transmit higher frequency signals (such as infrared and optical frequencies) as metallic wires experienced higher losses at these frequencies. On the contrary, the dielectric waveguides were subjected to dielectric absorption loss dependent on waveguide frequencies. Dielectric waveguides can be classified into two categories, which are hollow- and solid-core-fiber waveguides. The dielectric waveguides offer better light confinement capability than metallic waveguides, so the dielectric waveguides are more popular for terahertz wave propagation.

2. Photonic crystal fiber

In hollow-core dielectric waveguide, the light is confined by an omnidirectional mirror and the dielectric material is transparent to a high frequency signal. So that, the hollow-core dielectric waveguide eliminates the limitations existing in silica fiber and hollow metallic waveguide. The light-guiding mechanism in PCFs are exactly similar to the hollow-core dielectric waveguide so that the PCFs can be considered as a dielectric waveguide. The invention of photonic crystal fibers (PCFs) has opened a new door for optoelectronics researchers. However, the selection of the base material for PCF is a tough task as most of the materials experience wavelength-dependent attenuation loss for wide-band signals. In the recent past, a huge number of fused silica-based solid core optical waveguides have been theoretically and experimentally investigated due to some excellent characteristics of this material compared to other glasses or plastics [20]. Fused silica has higher tensile strength, higher transparency to light waves, lower absorption loss, higher availability in nature, high melting point, lower dispersion characteristics, and so on, which increase its popularity as an optical waveguide [21]. However, the silica-based fibers are not suitable for the terahertz spectrum as they offer high absorption loss and modal dispersion to terahertz signals. The most commonly used materials for terahertz dielectric waveguides are TOPAS, Zeonex, Teflon, PMMA, *etc*. due to their lower loss coefficients [15]. Among them, TOPAS and Zeonex offer the lowest loss coefficient and highest transparency towards the terahertz spectrum, so that various application dependent fiber waveguides based on those materials have been proposed [22].

PCFs can be classified into three categories on the basis of the core structure, which are solid core PCF [22], porous core PCF [23, 24], and hollow-core PCF [25]. In addition to wave communication functions, PCFs can also be used for optical sensing. To apply a PCF in sensing applications, the sample under test is filled in the core and after that, the electromagnetic wave is injected through the core [26]. The light interacts with the sample, and after analyzing the received signal, the unknown sample can be identified [26]. However, solid core PCF cannot be used in sensing applications as it is not possible to inject analyte inside of the solid core. So, numerous structures based on hollow-core and porous core dielectric fibers have been proposed as liquid or gas sensors [27–31] using the electromagnetic signal at 1.33 μm or 1.55 μm wavelengths. These proposed PCF-based sensors offer relatively

high sensitivity and superior guiding characteristics, which are compared with commonly used mechanical sensors and transducers.

3. PCF waveguide parameters

In order to claim a PCF as a good sensor, it must satisfy some criteria, including high relative sensitivity, low confinement loss, and high numerical aperture. The mathematical formulas or expressions are shown and explained, which are generally used to calculate the sensing and guiding characteristics of an optical sensor.

Relative sensitivity is the key parameter of any PCF-based sensor, which is an indication of how much change of an analyte can be sensed or detected by the sensor. Higher relative sensitivity is desirable from any sensor, as the higher the relative sensitivity, the smaller the change that can be identified by the sensor. The mathematical expression to calculate the relative sensitivity (r) is [27–34],

$$r = \frac{n_r}{n_{eff}} \times P\% \tag{1}$$

where n_r and n_{eff} are the effective refractive index of the actual propagating EM wave through the core and the analytes, respectively. In addition, P indicates how much light signal power interacts with the analytes filled in the fiber core. In the case of a PCF-based sensor, the parameter P is known as power fraction, and that can be easily calculated from the following mathematical expression [27],

$$P = \frac{\int_{sample} R_e\left(E_x H_y - E_y H_x\right) dxdy}{\int_{total} R_e\left(E_x H_y - E_y H_x\right) dxdy} \times 100 \tag{2}$$

where E_x, E_y, Hx, and H_y stand for x and y polarized electric field and magnetic field, respectively, when the propagation direction of light is in the z direction. The numerator of Eq. (2) integrates the energy that interacts with the sample under test and the denominator does the same for the complete sensor.

Another important propagation parameter for any kind of optical fiber-based waveguide or sensor is confinement loss. This loss parameter determines the actual fiber length as higher confinement loss restricts the actual fiber length. This parameter indicates the amount of power wastage due to the cladding air holes and it is usually calculated by employing the following expressions [27–29],

$$\alpha_{CL} = 8.686 \times \frac{2\pi f}{c} \mathrm{Im}\left(n_{eff}\right) \tag{3}$$

where f is the operating frequency of the propagating EM signal, c is the speed of light in free space, and Im (n_{eff}) stands for the imaginary part of the effective refractive index. In order to be considered a good sensor, the loss must be low. Till date, no optical sensor with lower confinement loss has been developed.

Along with the confinement loss, another loss is present in all optical sensors, which is called effective material loss (EML), which reflects the information power consumed by the background material of the sensor. However, many authors did not provide this parameter in their articles, but it is very important for the practical implementation or setup of a terahertz sensor. The mathematical equation to quantify the EML of a sensor is [1],

$$\alpha_{eff} = \frac{\left(\varepsilon_0/\mu_0\right)^{1/2}\int_{A_{mat}} n\ \alpha_{mat}|\mathrm{E}|^2 d\mathrm{A}}{2\int_{All} S_Z d\mathrm{A}} \tag{4}$$

where ε_0 and μ_0 indicate the relative permittivity and permeability of the vacuum, n is the refractive index of the guided light, and α_{mat} is the bulk material loss coefficient of the base material of the sensor. Usually, Topas and Zeonex are the most commonly used materials for the terahertz sensor as they provide the lowest loss coefficient in the terahertz regime. However, different terahertz sensors with PMMA, Teflon, *etc*. were also proposed by the researchers in the recent past which offered slightly higher EML than the recently proposed PCF-based sensors.

Another important propagation parameter is birefringence, which is important in the case of sensing applications. Birefringence is the absolute difference between the effective refractive indexes of x and y polarization mode which is expressed by using the following expression [32, 33],

$$B = \left|n_x - n_y\right| \tag{5}$$

where n_x and n_y are the effective refractive indexes in the x and y directions, respectively.

In addition, some other propagation characteristics such as bending loss, numerical aperture, V parameter, spot size, beam divergence, nonlinearity, *etc.* are discussed in [32–45].

4. Photonic-crystal-fiber-based terahertz sensor

A large number of PCF-based terahertz sensors have been proposed in the recent past for the identification of different types of chemicals [32–34], bane chemicals [41], blood components [48–50], alcohols [36], and so on. The prime designing objective of any kind of PCF-based sensor is to propagate the maximum amount of light through the core so that maximum light-analyte interaction takes place. The cross-sectional view of some excellent PCF-based sensors in the terahertz regime is represented in **Figure 1**.

A kagome lattice slotted core fiber is shown in **Figure 1(a)**, which was proposed by Islam *et al*. to detect benzene (n = 1.366), ethanol (n = 1.354), and water (n = 1.33) by using the terahertz spectrum [33]. The kagome structure in **Figure 1(a)** offers high confinement of light through the core due to the compact structure in the cladding. That's the reason why the proposed sensor in **Figure 1(a)** has high relative sensitivity in **Figure 2(a)** and **(b)** for the x and y polarization mode. As the core is not symmetrical, the power distribution in both polarization is unequal.

Another hybrid structured PCF with all rectangular holes is proposed by Islam *et al*. in order to detect three different liquids [37]. Its cross-section is shown in **Figure 1(b)** with an enlarged view of the core section. **Figure 1(b)** shows that the structure is not symmetric, performing birefringence and unequal power distribution in two polarization directions. The relative sensitivity is shown in **Figure 2(c)** and **(d)** for two different core dimensions. As the W value is larger than the H value, more light travels with the x-polarization mode. The sensitivity of a x-polarization mode is thus high. Similarly, **Figure 2(d)** shows the relative sensitivity increases as enlarging the fiber core.

Habib *et al*. proposed a simple hollow-core PCF-based chemical detector [40] using terahertz spectrum and the two-dimensional view is represented in

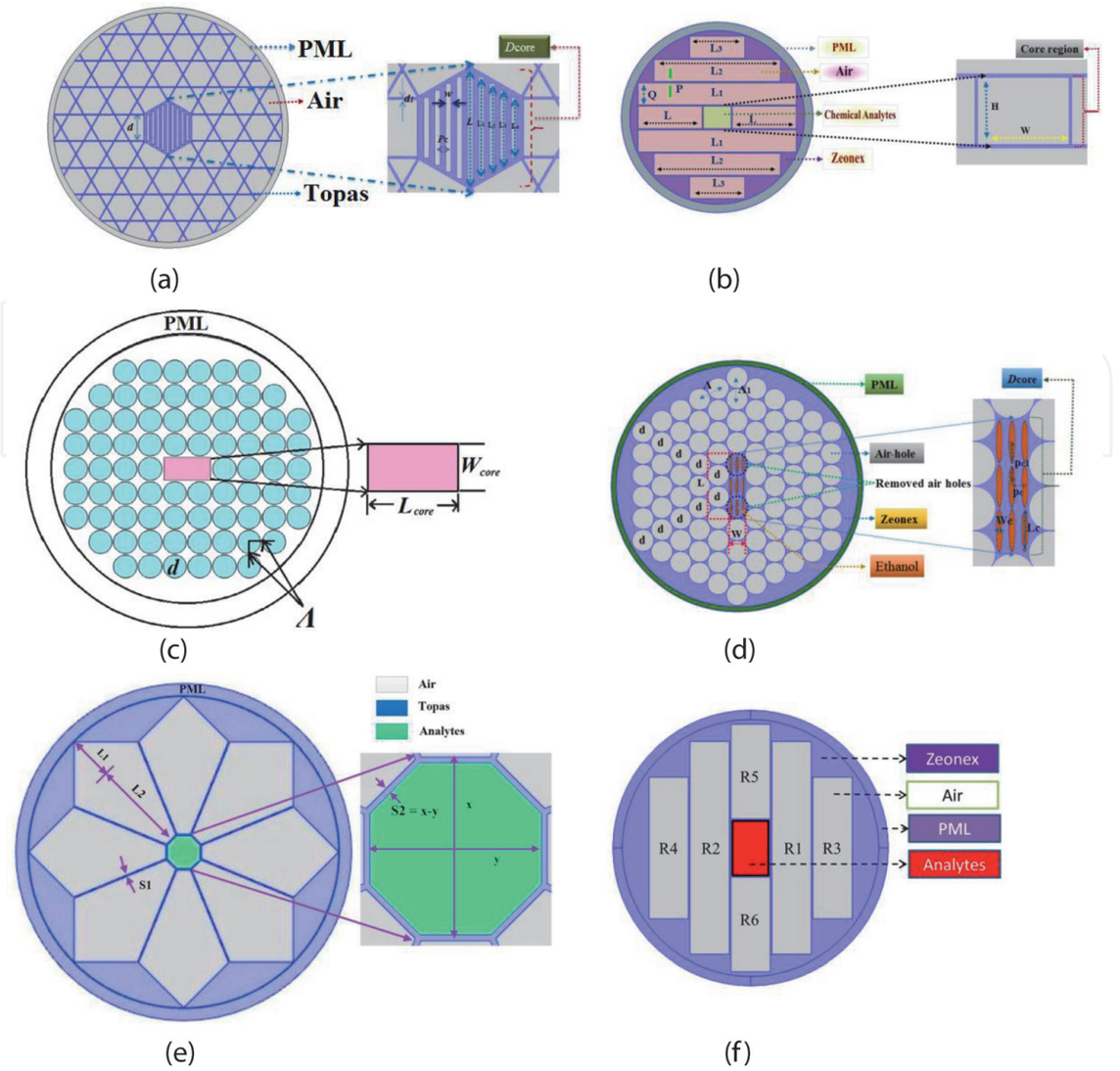

Figure 1.
Cross-sectional view of (a) kagome structured slotted core chemical sensor [33], (b) hybrid structured hollow-core chemical sensor [37], (c) hybrid structured rectangular hollow-core chemical sensor [40], (d) hexagonal structured rectangular porous core alcohol sensor [36], (e) hybrid structured polygonal hollow-core cholesterol sensor [45] and (f) hybrid structured rectangular hollow-core blood component sensor [48] in the terahertz regime.

Figure 1(c). One rectangular air hole is introduced in the core region to be injected by analytes. Due to asymmetric structure, this sensor also has birefringence and the relative sensitivity for both polarization modes are presented in **Figure 2(e)** and **(f)**. This sensor has extremely high sensitivity around 90% at 1.9 THz for the y-polarization mode.

A very simple hollow-core chemical sensor [36] was proposed in 2018 in **Figure 1(d)**. Due to the asymmetric core, the relative sensitivity of that sensor for both polarization modes is reported in **Figure 2(g)** and **(h)**. **Figure 1(d)** indicates that there are considerable amounts of high indexed solid material in the core region. This proposed sensor, therefore, extracts a small fractional THz signal for sensing and results in lower sensitivity. The maximum relative sensitivity is around 73% at 1 THz.

Figure 1(e) represents a hybrid structured hollow-core PCF [45] for the identification of cholesterol present in human blood and fruits. The proposed sensor offered a very high relative sensitivity of 98% at optimum conditions for two main reasons. Firstly, the hollow-core permits maximum light to travel through the core,

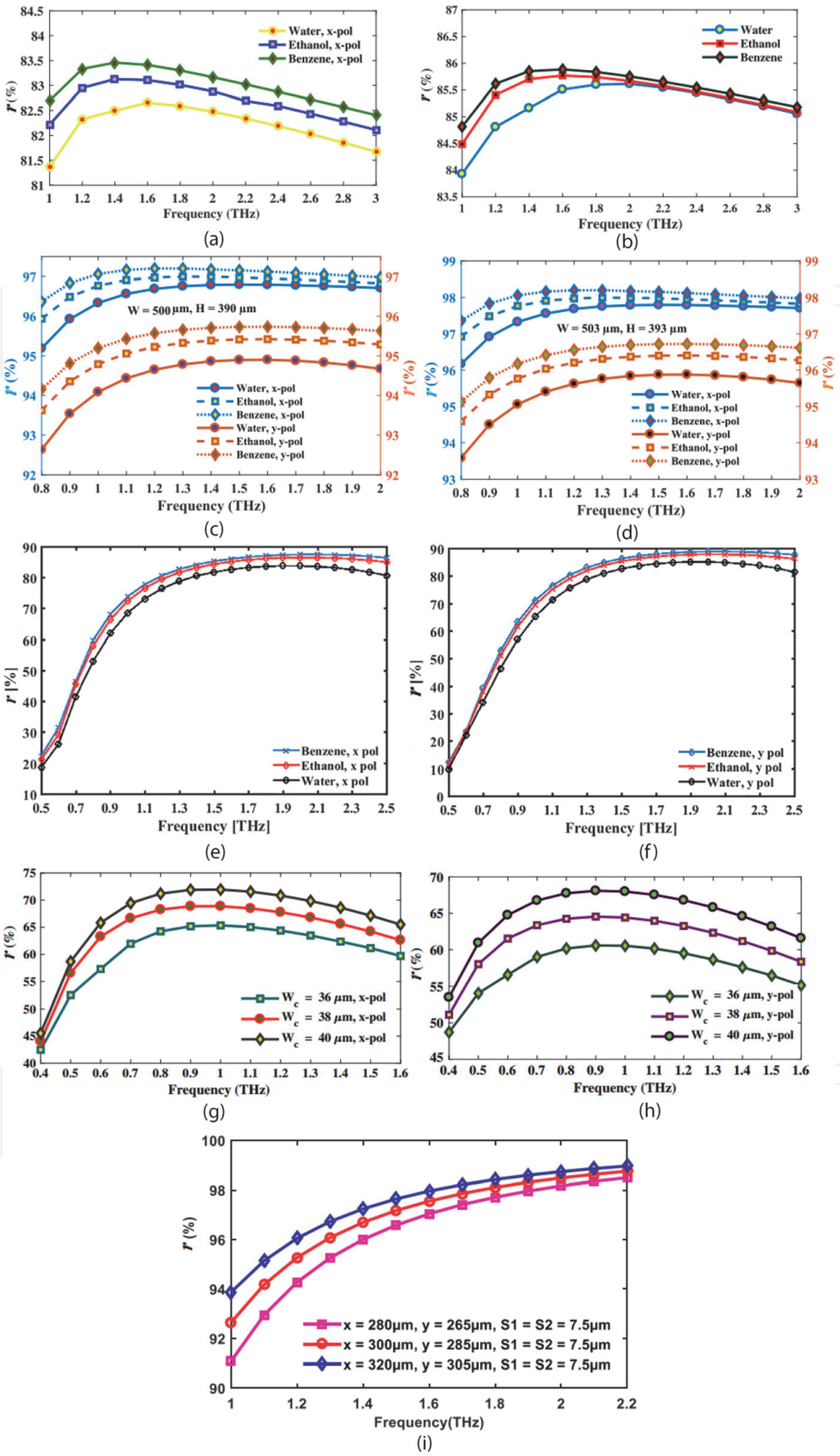

Figure 2.
Relative sensitivity of (a)-(b) kagome structured slotted core chemical sensor [33], (c)-(d) hybrid structured rectangular porous core chemical sensor [37], (e)-(f) hybrid structured rectangular hollow-core chemical sensor [40], (g)-(h) hexagonal structured rectangular porous core alcohol sensor [36], (i) hybrid structured polygonal hollow-core cholesterol sensor [45] for different operating frequencies in the terahertz regime.

which increases the power fraction, and finally, the higher refractive index cholesterol (n = 1.525) attracts more light to interact with itself. So that, according to the data of **Table 1**, the relative sensitivity of this cholesterol sensor is maximum and the graphical representation of the variation of relative sensitivity is shown in **Figure 2(g)**. This figure also shows the relationship between the core dimension and sensitivity. For example, the maximum core dimension has the highest relative sensitivity than at 1.2 THz when the enlarged core has strong light-analyte interaction.

Few PCF-based sensors can identify different components of human blood [48–50]. In 2019, Ahmed *et al*. proposed a hollow-core Zeonex-based blood component sensor in the terahertz spectrum [48], whose cross-sectional view is represented in **Figure 1(f)**. The relative sensitivity of red blood cells (RBCs), hemoglobin, white blood cells (WBCs), plasma, and water for different operating frequencies is shown in **Figure 3(a)** and **(b)**. From the above discussion, it is clear that the relative sensitivity of the terahertz sensors is higher than the silica-based sensors using IR spectrum [27–31]. In addition, hollow-core terahertz sensors offer higher sensitivity (**Figure 2(c)–(f), (i)**) than that of porous core sensors (**Figure 2(a), (b), (g), (h)**).

Now, the loss characteristics of different types of terahertz PCF sensors are discussed below. To reduce the confinement loss and the effective material loss, numerous types of core and cladding structured PCFs were presented [26, 32–35]. However, the light confinement inside the core is largely dependent on the geometric structure of PCF. Now, the variation of confinement loss of PCF-based sensors (**Figure 1**) for different THz frequencies is shown in **Figure 4(a)–(f)**. The first three figures (**Figure 4(a)–(c)**) represent the confinement loss characteristics at certain PCF structures for sensing benzene, ethanol, and water [33, 37, 40]. At high THz frequency, the confinement loss is lower for all analytes because a few fractional THz wave at high frequency travels through the cladding air holes. The confinement loss of benzene is lowest than the other two samples due to the highest refractive index. The sensing results of **Figure 1(d)** and **(e)** are represented in **Figure 4(d)** and **(e)** respectively. The two figures inform that the loss is inversely proportional to the core dimension of the PCFs. Finally, **Figure 4(f)** shows the confinement loss for sensing blood samples [48]. The confinement loss is low at the high THz frequency and high refractive index conditions. THz waves with high frequencies have the tendency to travel through the high indexed zone, so less fractional power propagates through the cladding. The confinement loss is low at high THz frequencies for all PCF-based sensors. The confinement loss is minimum for the cholesterol sensor (**Figure 1(e)**).

Now, the THz wave loss characteristics of different PCF-based sensors in the terahertz regime are investigated. The THz loss spectra are represented in **Figure 5** for different proposed terahertz sensors shown in **Figure 1(a)–(f)**. This loss comes from the solid materials around the core. The THz wave loss characteristics of benzene, ethanol, and water sensors in **Figure 1(b)** and **(c)** are shown in **Figure 5(a)** and **(b)** for different operating frequencies. However, according to **Figure 5(a)** and **(b)**, it is clear that the loss shows an upward trend with the increase of operating frequency. Because THz waves at higher frequency can travel through high indexed solid material, the material more absorbs THz wave energy. **Figure 5(c)** and **(d)** represent THz wave loss characteristics of PCF-based sensors in **Figure 1(d)** and **(e)** for different structural conditions. **Figure 5(c)** shows that THz wave loss is lower for increasing the width of elliptical air holes (**Figure 1(e)**). **Figure 5(d)** shows that the THz wave loss is lowest for the largest core dimension. This structure in **Figure 5(d)** performs the lowest loss among **Figure 5(a)–(d)**.

Ref.	Sensor's structure	Sample's name	r[%]	α_{CL}[dB/m]	α_{eff} [cm^{-1}]	B
[32]	Cladding- Hexagonal Core- Hexagonal Material: Topas	Ethanol	73.5	N/A	N/A	0.011
		Water	71.5	N/A	N/A	0.013
[33]	Cladding- kagome Core- slotted Material: Topas	Benzene	85.9	1.02×10^{-9}	N/A	0.0065
		Ethanol	85.7	1.7×10^{-9}	N/A	0.005
		Water	85.6	4.5×10^{-9}	N/A	0.0043
[34]	Cladding- Hybrid Core- circular Material: Topas	Benzene	78.8	5.83×10^{-9}	N/A	N/A
		Ethanol	78.5	5.81×10^{-10}	N/A	N/A
		Water	69.7	5.34×10^{-8}	N/A	N/A
[35]	Cladding- Hybrid Core- Hybrid Material: Zeonex	HCN	77.5	4.34×10^{-8}	N/A	0.049
		KCN	85.7	4.34×10^{-8}	N/A	0.042
		NACN	87.6	4.34×10^{-8}	N/A	0038
[36]	Cladding- Hexagonal Core- Rectangular Material: Zeonex	Ethanol	68.87	2.66×10^{-9}	0.05	0.0176
[37]	Cladding- Slotted Core- Rectangular Material: Zeonex	Benzene	97.2	1.5×10^{-11}	N/A	0.019
		Ethanol	96.97	3.02×10^{-11}	N/A	0.017
		Water	96.6	2.7×10^{-12}	N/A	0.015
[38]	Cladding- circular Core- circular Material: Silica	Benzene	77.16	1.39×10^{-7}	N/A	N/A
		Ethanol	76.44	1.43×10^{-7}	N/A	N/A
		Water	73.20	1.49×10^{-7}	N/A	N/A
[39]	Cladding-Heptagonal Core- rotated hexa Material: Topas	Benzene	63.24	10^{-10}	N/A	N/A
		Ethanol	61.05	10^{-10}	N/A	N/A
		Water	60.03	10^{-10}	N/A	N/A
[40]	Cladding- Hybrid Core- rectangular hollow Material: Zeonex	Benzene	89	1.15×10^{-7}	N/A	0.007
		Ethanol	88	1.15×10^{-7}	N/A	0.007
		Water	86	1.15×10^{-7}	N/A	0.007
[41]	Cladding- Hexagonal Core- quad elliptical Material: Zeonex	Tabun	63.7	4.34×10^{-5}	0.033	N/A
		Sarin	64.4	4.34×10^{-5}	0.028	N/A
[42]	Cladding- Hybrid Core- rectangular Material: Zeonex	Tabun	95.5	7.42×10^{-12}	0.0094	0.006
		Soman	94.87	9.33×10^{-12}	0.0089	0.00645
		Sarin	94.28	1.24×10^{-11}	0.0086	0.068
[43]	Cladding-Heptagonal Core- rotated hexa Material: Silica	Benzene	69.20	1.92×10^{-9}	N/A	N/A
		Ethanol	68.48	2.13×10^{-9}	N/A	N/A
		Water	66.7	2.7×10^{-6}	N/A	N/A
[44]	Cladding- Hexagonal Core- rotated hexa Material: Topas	Benzene	82.26	6×10^{-8}	N/A	N/A
		Ethanol	81.46	5.85×10^{-8}	N/A	N/A
		Water	79.22	5.84×10^{-8}	N/A	N/A
[45]	Cladding- Eight head star Core- octagonal Material: Topas	Cholesterol	98.75	1.34×10^{-17}	0.0008	N/A

Ref.	Sensor's structure	Sample's name	r[%]	α_{CL}[dB/m]	α_{eff} [cm^{-1}]	B
[46]	Cladding- Hybrid Core- slotted Material: Topas	Benzene	93.95	4.08×10^{-9}	0.0125	N/A
		Water	93.70	2.66×10^{-8}	0.0118	N/A
		HCN	93.40	4.08×10^{-9}	0.0100	N/A
		NaCN	9442	3.77×10^{-6}	0.0149	N/A
		Ketamine	94.87	3.97×10^{-7}	0.0175	N/A
		Amphetamine	94.78	3.17×10^{-6}	0.0165	N/A
[47]	Cladding- Octagonal Core- rotated hexa Material: Topas	Benzene	78.06	3.02×10^{-6}	N/A	N/A
		Ethanol	77.14	2.26×10^{-3}	N/A	N/A
		Water	76.11	2.72×10^{-2}	N/A	N/A
[48]	Cladding-Rectangular slotted Core- Rectangular hollow Material: Zeonex	RBC	93.5	1.35×10^{-11}	N/A	N/A
		HB	92.41	2.16×10^{-11}	N/A	N/A
		WBC	91.25	3.26×10^{-11}	N/A	N/A
		Plasma	90.48	3.95×10^{-11}	N/A	N/A
		Water	89.14	5.64×10^{-11}	N/A	N/A
[49]	Cladding- Hybrid Core- Hybrid Material: Topas	RBC	80.93	1.23×10^{-11}	N/A	N/A
		HB	80.56	8.63×10^{-12}	N/A	N/A
		WBC	80.13	4.93×10^{-12}	N/A	N/A
		Plasma	79.91	2.93×10^{-12}	N/A	N/A
		Water	79.39	1.30×10^{-12}	N/A	N/A
[50]	Cladding- Hexagonal Core- Hybrid Material: Zeonex	RBC	83.45	2.91×10^{-13}	N/A	N/A
		HB	81.20	4.05×10^{-13}	N/A	N/A
		WBC	80.78	8.2×10^{-13}	N/A	N/A
		Plasma	79.60	4.92×10^{-12}	N/A	N/A
		Water	78.80	3.49×10^{-12}	N/A	N/A
[51]	Cladding-Hybrid Core-Circular Material: Zeonex	RBC	95.80	3.80×10^{-11}	N/A	N/A
		HB	95	1.13×10^{-11}	N/A	N/A
		WBC	93.6	2.15×10^{-10}	N/A	N/A
		Plasma	92.5	6.25×10^{-10}	N/A	N/A
		Water	91.4	8.30×10^{-9}	N/A	N/A

Table 1.
Comparison of different guiding and sensing parameters for numerous types of remarkable terahertz sensors.

The following comparison shows the guiding characteristics for hybrid structured sensors [34, 35, 40, 42, 46, 48] and conventional structured sensors [33, 36–39, 41, 43–45, 47, 49–51] in terahertz regime.

The most interesting characteristic of PCF-based sensors is that the guiding or sensing properties are highly dependent on the geometry or structure of the PCFs. However, from **Table 1**, it is quite clear that the relative sensitivity and loss profile is lower for nonconventional structured PCF than regular structured one. For example, the conventional structured liquid sensor in Ref. [44] offered the highest sensitivity of 82.26% among regular structured PCFs but the core loss is high (>10 dB^{-8} dB/m). On the other hand, a maximum of 93.5% relative sensitivity with

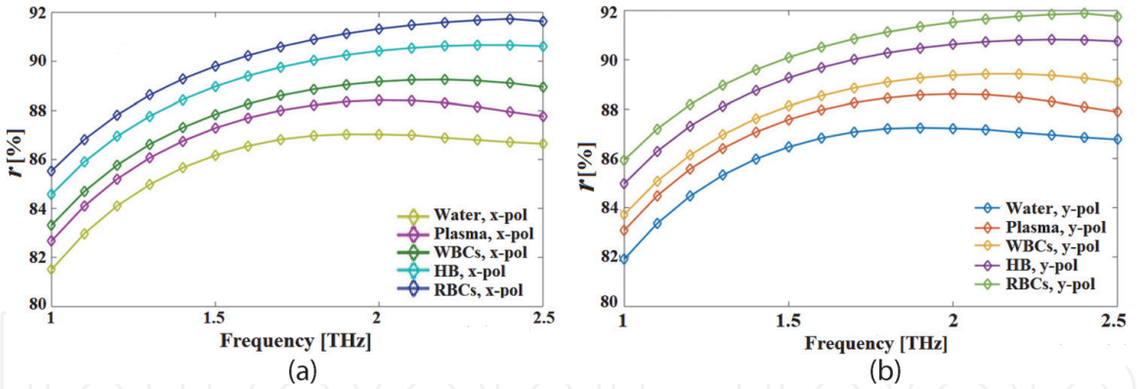

Figure 3.
Relative sensitivity as a function of frequency for different blood components in terahertz regime from (a)-(b) in ref. [48].

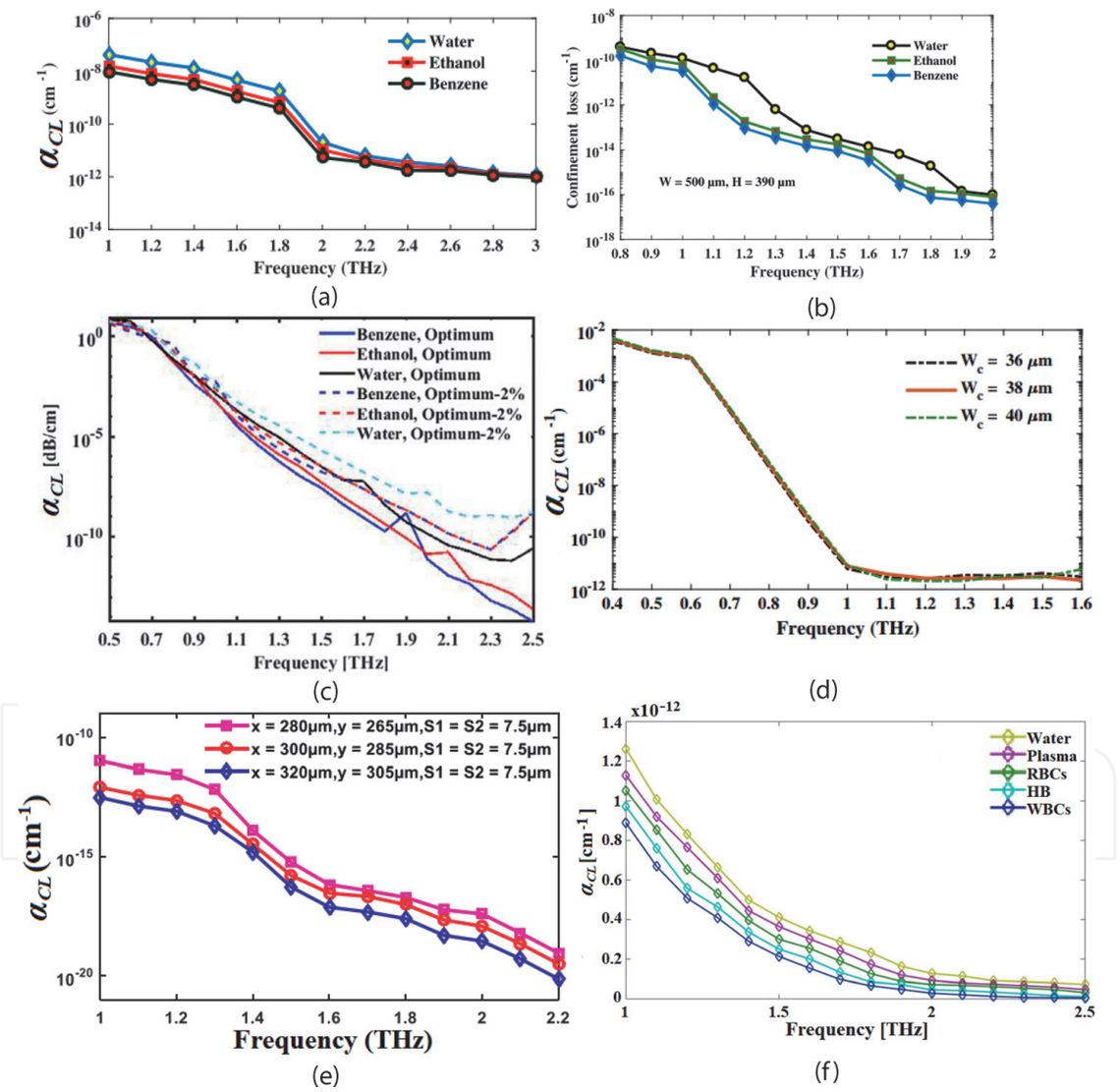

Figure 4.
*Confinement loss as a function of frequency of (a) **Figure 1(a)** ref. [33], (b) **Figure 1(b)** ref. [37], (c) **Figure 1(c)** ref. [40], (d) **Figure 1(d)** ref. [36], (e) **Figure 1(e)** ref. [45] and (f) **Figure 1(f)** ref. [48] for different PCF based sensors.*

lower confinement loss (< 10 dB^{-9} dB/m) can be achieved from PCF-based sensor in Ref. [46]. Moreover, the relative sensitivity and loss are also dependent on the test sample also. In **Table 1** the highest relative sensitivity (98.75%) and lowest loss

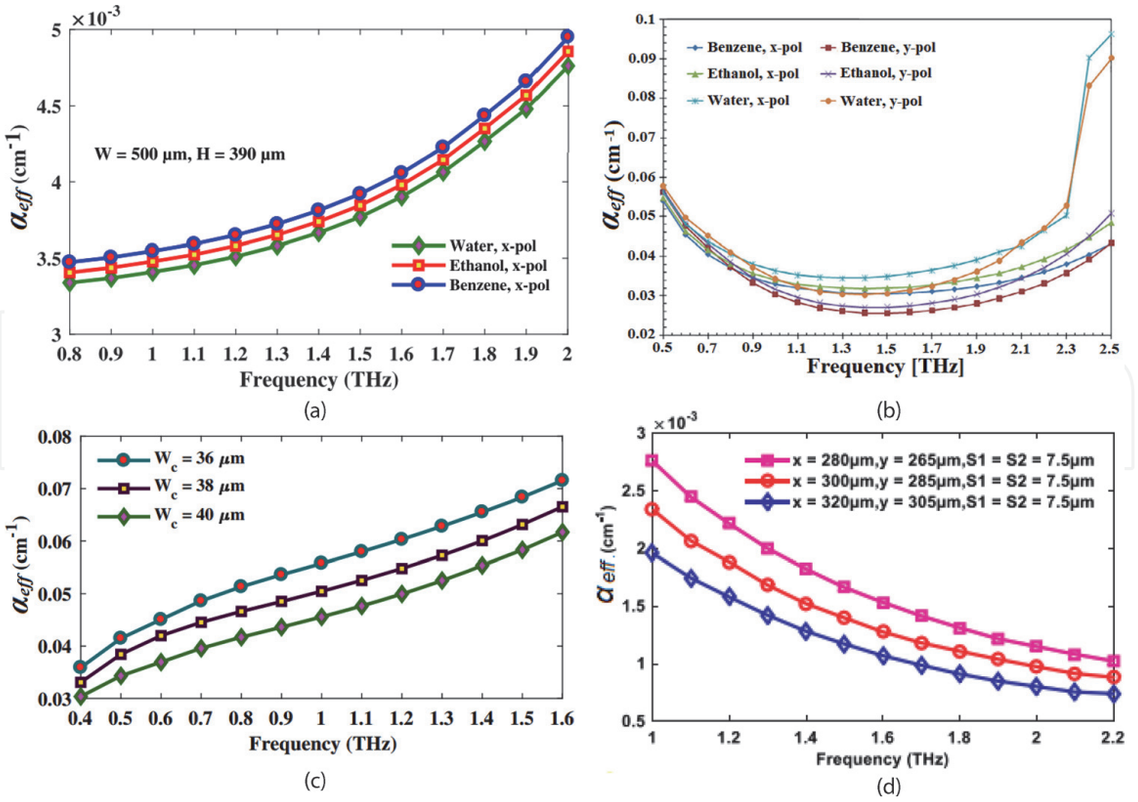

Figure 5.
Effective material loss variation of numerous structured terahertz sensorsas a function of frequency of (a) ***Figure 1(b)*** *ref. [37], (b)* ***Figure 1(c)*** *ref. [40], (c)* ***Figure 1(d)*** *ref. [36], (d)* ***Figure 1(e)*** *ref. [45].*

(core loss = 1.34 × 10 dB^{-17} dB/m and THz wave loss = 0.008 cm^{-1}) was reported in Ref. [45] as the refractive index of cholesterol (refractive index = 1.525) is maximum than any other samples reported in **Table 1**.

5. Conclusion

In this chapter, different types of PCF-based terahertz sensors were discussed and compared for numerous chemicals, toxic agents, and blood components identification. In addition, a brief discussion about terahertz technology and different terahertz waveguides are included in this chapter. The sensing and guiding parameters of numerous terahertz sensors are numerically discussed and graphically represented for a better understanding of the readers. However, efficient application-specific terahertz sensors are still under research and we hope this chapter will help the optoelectronics researchers to propose new sensors.

Author details

Md. Ahasan Habib[1*], Md. Shamim Anower[1] and Md. Nazmul Islam[2]

1 Department of Electrical and Electronic Engineering, Rajshahi University of Engineering and Technology, Rajshahi, Bangladesh

2 Department of Electrical and Electronic Engineering, Bangabandhu Sheikh Mujibur Rahman Science and Technology University, Gopalganj, Bangladesh

*Address all correspondence to: habib.eee.116.ah@gmail.com

References

[1] Ahlbom A, Bridges J, Seze R, Hillert L, Juutilainen J, Mattsson M, et al. Possible effects of electromagnetic fields (EMF) on human health—Opinion of the Scientific Committee on Emerging and Newly Identified Health Risks (SCENIHR). Toxicology. 2008;**246**:248-250

[2] Yang X, Zhao X, Yang K, Liu Y, Fu W, Luo Y. Biomedical applications of terahertz spectroscopy and imaging. Trends in Biotechnology. 2016;**34**(10): 810-824

[3] Habib MA, Anower MS. Design and numerical analysis of highly birefringent single mode fiber in THz regime. Optical Fiber Technology. 2009;**47**:197-203

[4] Reza MS, Habib MA. Extremely sensitive chemical sensor for terahertz regime based on a hollow core photonic crystal fiber. Ukrainian Journal of Physical Optics. 2020;**21**(1):8-14

[5] Zhang XC. Terahertz wave imaging: Horizons and hurdles. Physics in Medicine & Biology. 2002;**47**(21):3663

[6] Wu K, Qi C, Zhu Z, Wang C, Song B, Chang C. Terahertz wave accelerates DNA unwinding: A molecular dynamics simulation study. Journal of Physical Chemistry Letters. 2020;**11**(17):7002-7008

[7] Song Q, Zhao Y, Redo-Sanchez A, Zhang C, Liu X. Fast continuous terahertz wave imaging system for security. Optics Communications. 2009; **282**(10):2019-2022

[8] Zhang Z, Ding H, Yang X, Liang L, Wei D, Wang M, et al. Sensitive detection of cancer cell apoptosis based on the non-bianisotropicmetamaterial biosensors in terahertz frequency. Optical Material Express. 2018;**8**(3):659-667

[9] Cheon H, Paik JH, Choi M, Yang H, Son J. Detection and manipulation of methylation in blood cancer DNA using terahertz radiation. Scientific Reports. 2019;**9**(6413)

[10] Cooper KB, Dengler RJ, Liombart N, Bryllrt T, Chattopadhyay G, Mehdi I, et al. An approach for sub-second imaging of concealed objects using terahertz radar. Journal of Infrared Millimeter, Terahertz and Waves. 2009;**30**:1297-1307

[11] Shrekenhamer D, Watts C, Padilla W. Terahertz single pixel imaging with an optically controlled dynamic spatial light modulator. Optics Express. 2013;**21**(10): 12507-12518

[12] Lewis RA. A review of terahertz sources. Journal of Physics: D. 2014;**47**: 374001

[13] Yardimci NT, Cakmakyapan S, Hemmati S, Jarrahi M. A high power broadband terahertz source enabled by three dimensional light confinement in a plasmonic nanocavity. Scientific Reports. 2017;**7**:4166

[14] McGowan RW, Gallot G, Grischkowsky D. Propagation of ultra-wideband short pulses of THz radiation through sub millimeter-diameter circular waveguides. Optics Letters. 1999;**24**:1431-1433

[15] Atakaramians S. Terahertz waveguides: A study of microwires and porous fibers. Available from: http://hdl.handle.net/2440/69317. 2011

[16] Gallot G, Jamison SP, McGowan RW, Grischowsky D. Terahertz waveguides. Journal of Optical Society of America B. 2000;**17**(5):851-863

[17] Mendis R, Grischkowsky D. Undistorted guided wave propagation of sub picosecond terahertz pulses. Optics Express. 2001;**26**(11):846-848

[18] Wang K, Mittleman DM. Metal wires for terahertz wave guiding. Nature. 2004;**432**:376-379

[19] Wachter M, Nagel M, Kurz H. Metallic slit waveguide for dispersion free low loss terahertz signal transmission. Applied Physics Letter. 2007;**90**:061111

[20] Kuhlmey BT, Eggleton BJ, Wu DKC. Fluid filled solid-core photonic bandgap fibers. Journal of Lightwave Technology. 2009;**27**(11):1617-1630

[21] You J, Lin S, Zhang J, Lin S, Fu L, Zheng R, et al. Optical properties of He^+ implanted fused silica glass waveguides. International Journal of Modern Physics B. 2021;**35**(2):2150026

[22] Sterke CM, Grujic T, Kuhlmey BT, Argyros A. Solid core photonic crystal fiber with ultrawide bandgap. Frontiers in Optics. 2020. DOI: 10.1364/FIO.2010.FTuW2

[23] Habib MA, Anower MS, Hasan MR. Highly birefringent and low effective material loss microstructure fiber for terahertz wave guidance. Optics Communications. 2018;**423**:140-144

[24] Habib MA, Anower MS. Square porous core microstructure fiber for low loss terahertz applications. Optics and Spectroscopy. 2019;**126**(5):607-613

[25] Couny F, Benabid F, Light PS. Large pitch kagome structured hollow core photonic crystal fiber. Optics Letters. 2006;**31**(24):3574-3576

[26] Habib MA, Vera ER, Aristizabal JV, Anower MS. Numerical modelling of a rectangular hollow core waveguide for the detection of fuel adulteration in terahertz region. Fibers. 2020;**8**:63

[27] Asaduzzaman S, Ahmed K, Bhuiyan T, Farah T. Hybrid photonic crystal fiber in chemical sensing. Springer Plus. 2016;**5**:748

[28] Paul BK, Ahmed K, Asaduzzaman S, Islam MS. Folded cladding porous shaped photonic crystal fiber with high sensitivity in optical sensing applications: Design and analysis. Sensing and Bio-Sensing Research. 2017;**12**:36-42

[29] Podder E, Hossain MB, Jibon RH, Bulbul AAM, Mondal HS. Chemical sensing through photonic crystal fiber: Sulfuric acid detection. Frontiers in Optoelectronics. DOI: 10.1007/s12200-019-0903-8

[30] Leon MJBM, Abedin S, Kabir MA. A photonic crystal fiber for liquid sensing applications with high sensitivity, birefringence and low confinement loss. Sensors International. DOI: 10.1016/j.sintl.2020.100061

[31] Eid MMA, Habib MA, Anower MS, Rashed ANZ. Highly sensitive nonlinear photonic crystal fiber based sensor for chemical sensing applications. Microsystem Technologies. DOI: 10.1007/s00542-020-05019-w

[32] Rana S, Kandadai N, Subbaraman H. A highly sensitive polarization maintaining photonic crystal fiber sensor operating in the THz regime. Photonics. 2018;**5**(40):1-9

[33] Islam MS, Sultana J, Ahmed K, Islam MR, Dinovitser A, Ng BW, et al. A novel approach for spectroscopic chemical identification using photonic crystal fiber in the terahertz regime. IEEE Sensors Journal. 2018;**18**(2):575-582

[34] Paul BK, Ahmed K, Vigneswaran D, Ahmed F, Roy S, Abbott D. Quasi photonic crystal fiber based spectroscopic chemical sensor in the Terahertz spectrum: Design and analysis. IEEE Sensors Journal. 2018;**18**(24):9948-9954

[35] Islam MS, Sultana J, Dinovitser A, Ng BW, Abbott D. Sensing of toxic chemicals using polarized photonic crystal fiber in terahertz regime. Optics Communications. 2018;**426**:341-347

[36] Sultana J, Islam MS, Ahmed K, Dinovitser A, Ng BW, Abbott D. Terahertz detection of alcohol using a photonic crystal fiber sensor. Applied Optics. 2018;**57**(10):2424-2433

[37] Islam MS, Sultana J, Rifat AA, Dinovitser A, Ng BW, Abbott D. Terahertz sensing in a hollow core photonic crystal fiber. IEEE Sensors Journal. 2018;**18**(10):4073-4080

[38] Sen S, Ahmed K. Design of terahertz spectroscopy based optical sensor for chemical detection. SN Applied Sciences. 2019;**1**:1215

[39] Hasan MM, Sen S, Rana MJ, Paul BK, Habib MA, Daiyan GM, et al. Heptagonal photonic crystal fiber based chemical sensor in THz regime. In: Joint 2019 8th International Conference on Informatics, Electronics & Vision (ICIEV) & 3rd International Conference on Imaging, Vision & Pattern Recognition (IVPR).

[40] Habib MA, Anower MS, Abdulrazak LF, Reza MS. Hollow core photonic crystal fiber for chemical identification in terahertz regime. Optical Fiber Technology. 2019;**52**:101933

[41] Yakasai I, Abas PE, Kaijage SF, Caesarendra W, Begu F. Proposal for a quad-elliptical photonic crystal fiber for terahertz wave guidance and sensing chemical warfare liquids. Photonics. 2019; **6**:78

[42] Hossain MB, Podder E, Bulbul AA, Mondal HS. Bane chemical detection through photonic crystal fiber in terahertz regime. Optical Fiber Technology. 2020;**54**:102102

[43] Hossain MS, Sen S. Design and performance improvement of optical chemical sensor based photonic crystal fiber (PCF) in the Terahertz (THz) wave propagation. SILICON. DOI: 10.1007/s12633-020-00696-8

[44] Sen S, Shafi MAA, Kabir MA. Hexagonal photonic crystal Fiber (H-PCF) based optical sensor with high relative sensitivity and low confinement loss for terahertz (THz) regime. Sensing and Bio-Sensing Research. 2020;**30**: 100377

[45] Rahman MM, Mou FA, Bhuiyan MIH, Islam MR. Photonic crystal fiber based terahertz sensor for cholesterol detection in human blood and liquid foodstuffs. Sensing and Bio-Sensing Research. 2020;**29**:100356

[46] Rahman A, Khaleque A, Ali MY, Rahman MT. THz spectroscopic sensing of liquid chemicals using a photonic crystal fiber. OSA Continuum. 2020; **3**(11):2982-2996

[47] Shafi MAA, Sen S. Design and analysis of a chemical sensing octagonal photonic crystal fiber (O-PCF) based optical sensor with high relative sensitivity for terahertz (THz) regime. Sensing and Bio-Sensing Research. 2020;**29**:100372

[48] Hossain MB, Podder E. Design and investigation of PCF-based blood components sensor in terahertz regime. Applied Physics A. 2019;**125**:861

[49] Ahmed K, Ahmed F, Roy S, Paul BK, Akter MN, Vigneswaran D, et al. Refractive index based blood components sensing in Terahertz spectrum. IEEE Sensors Journal. 2019; **19**(9):3368-3375

[50] Habib MA. A refractive index based micro-structured sensor forblood components detection in terahertz regime. Sensor Letters. 2020;**18**(1):74-81

[51] Eid MMA, Habib MA, Anower MS, Rashed ANZ. Hollow core photonic crystal fiber (PCF)–based optical sensor for blood component detection in Terahertz spectrum. Brazilian Journal of Physics. 2021;**51**:1017-1025